J. Membrane Biol. 128, 91–102 (1992)

The Journal of
Membrane Biology

Single-Membrane and Cell-to-Cell Permeability Properties of Dissociated Embryonic Chick Lens Cells

A.G. Miller†, G.A. Zampighi‡, and J.E. Hall†

†Department of Physiology and Biophysics, University of California at Irvine, Irvine, California 92715, and ‡Department of Cell Biology and Anatomy, University of California at Los Angeles, Los Angeles, California 90024

Summary. Ion channels are believed to play an important role in the maintenance of lens transparency. In order to ascribe junctional and nonjunctional permeability properties to specific lens cell types, embryonic chick lenses were enzymatically dissociated into cell clusters, cell pairs and single cells, and both cell-to-cell and single-membrane permeability properties were characterized with the patch-clamp technique. Double patch-clamp experiments and single patch-clamp experiments with Lucifer yellow in the pipette demonstrated that the cells in the dissociated preparation were well coupled, the average conductance between pairs being 42 ± 27 nS. Double patch-clamp experiments also revealed single cell-to-cell channel events with a predominant unitary conductance of 286 ± 38 pS. Whole-cell measurements of surface membrane conductance indicate heterogeneity within the population of dissociated embryonic chick lens cells: 63% of the cells have a voltage-independent leak current, 14% of the cells have a potassium-selective inward-rectifier current, and 23% of the cells have a current which turns off with positive voltage on a time scale on the order of seconds. The time constant for this turnoff is voltage dependent.

Key Words lens · embryonic · gap junctions · ion channels

Introduction

The lens is a transparent avascular syncytium composed of two main cell types. In the adult lens, a single layer of cells, the anterior epithelium, covers a regularly packed mass of thin, elongated fiber cells. These fiber cells originate from the anterior epithelium by terminal differentiation and comprise the bulk of the lens tissue (Fig. 1). The epithelial cells contain the normal complement of organelles as well as active pump mechanisms, whereas the majority of fiber cells have lost most, if not all, of their organelles and contain relatively little active pumping capacity (Unakar & Tsui, 1980).

The primary role of the lens is to focus light onto the retina. In order to accomplish this the lens must be transparent. At present the cellular mechanisms behind maintenance of lens transparency are not well understood. However, experimental evidence links changes in membrane permeability to the formation of one type of cataract (Patmore & Duncan, 1981; Bunce, Kinoshita & Horwitz, 1990). Lenses soaked in ouabain, which inhibits the Na^+–K^+ ATPase, or in abnormal levels of calcium, which alters lens membrane permeability, form cataracts (Shinohara & Piatigorsky, 1977; Duncan & Jacob, 1984). Also changes in internal lens sodium, potassium, calcium, and chloride concentrations have been associated with certain types of cataracts (Duncan & Bushell, 1975; 1979; Shinohara & Piatigorsky, 1977). The manner in which lens cells maintain ionic homeostasis is important for lens transparency, and therefore a study of the number and type of ionic channels found in different types of lens cells is likely to be of considerable value in understanding cataract formation.

The experimental evidence that ionic conductances are important in the lens is supported by a theoretical model developed by Mathias and Rae (Mathias & Rae, 1985*a*,*b*; Mathias et al., 1985) which provides a putative role for fluid balance in maintaining transparency in the lens. This model proposes that different membrane ionic permeabilities at different regions in the lens give rise to circulating chloride and sodium currents. These currents in turn give rise to a water flux which could serve to bring nutrients deep inside the lens and to remove harmful waste products.

This model is supported by impedance studies on whole lenses which indicate that inner fiber membranes are predominantly permeable to chloride and sodium and that the surface membranes are predominantly permeable to potassium (Mathias et al., 1985). Also, vibrating probe current measurements show a net outward flux of potassium at the equator and a net inward flux of sodium at the poles

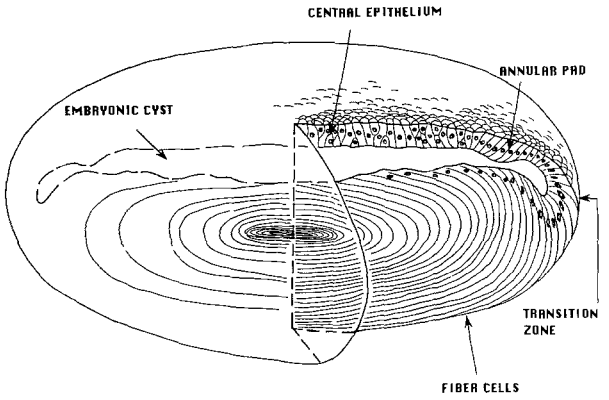

Fig. 1. A schematic drawing of a 14-day-old embryonic chick lens. For emphasis, some features are not drawn to scale.

(Robinson & Patterson, 1983; Wind, Walsh & Patterson, 1988).

Experiments on isolated lens cells can reveal membrane conductances inaccessible to whole-lens electrophysiology. Detailed single-membrane and cell-to-cell permeability properties of individual cells from different regions within the lens can be studied. Thus, in principle, it is possible to assign specific permeability properties such as channel conductance, channel selectivity and number of channels to specific cell types in the lens. The electrophysiological profile generated would thus allow evaluation of the proposed model and provide data necessary for refining it. It would also allow a comparison with the electrophysiological profile from cataractous lenses.

Numerous patch-clamping and microelectrode voltage-clamping studies have been performed on cultured lens epithelial cells from a variety of species (Jacob, 1986; Stewart et al., 1988; Cooper et al., 1990), on peeled-off epithelia layers from adult frog lens (Rae & Levis, 1984; Jacob, Bangham & Duncan, 1985; Rae, 1985, 1986; Cooper et al., 1986; Duncan et al., 1988), on fiber cells remaining after removal of the epithelial layer (Rae, 1985), and recently on dissociated adult frog epithelial cells (Cooper, Rae & Gates, 1989). These experiments show that epithelial cells are coupled via gap junction channels and that while there are differences in channel properties between species, lens epithelial cells are dominated by a potassium conductance, features consistent with the model of ion and water fluxes proposed by Mathias and Rae (1985*a*). In addition, there are differences in lens channel properties between embryonic and adult lenses of the same species (Rae & Cooper, 1989; Rae et al., 1990).

To provide data for modeling and species comparison, we have used whole-cell patch clamping to characterize single-membrane and cell-to-cell conductances of dissociated embryonic chick lens cells. Embryonic lenses are in a continual state of differentiation and therefore contain, in addition to epithelial and fiber cells, cells which are in the process of differentiating from epithelial cell to fiber cell. At present it is not clear what membrane properties these cells would have. Thus this dissociated preparation offers a range of cell types, each with possibly different electrophysiological properties. Part of this work has been previously presented in abstract form (Miller, Hall & Zampighi, 1990).

Materials and Methods

Cell Preparation

Lenses were removed from 9–15 day Hypeco Bovans W1 embryos. Cells were obtained by a slight modification of the method used by Menko et al. (1987). Briefly, 10 to 15 lenses were removed from the vitreous humor and placed in a 10-ml conical tube with 0.08% trypsin solution at 37°C (4 ml trypsin dissociation buffer (TD), 2 ml 0.25% lyophilized trypsin, Gibco Laboratories, Life Technologies, Grand Island, NY) for 15 min. The trypsin solution was aspirated off and replaced with a fresh 0.08% trypsin solution identical to the first trypsin solution in order to aid in removal of vitreous humor and zonules attached to the lenses. Older lenses (14–15 days) were easier to clean than younger lenses (9–10 days). The lenses were left in the second trypsin solution for 15 min with continual mechanical agitation of the tube for the last 5 min. At this time most of the lenses were broken up into small pieces. The dissociated lenses were spun at 102 RCF for 15 min in a Technospin centrifuge. The cells were then resuspended in 3 ml of Medium 199 with 10% fetal calf serum and incubated at 37°C with 5% CO_2 for 2–10 hr. Just before a given set of patch-clamp experiments, 50 μl of cell suspension were plated out onto a glass chamber coated with 100 μg/ml poly-D-lysine.

Dye Measurements

Patch pipettes were filled with concentrations of Lucifer yellow (mol wt 457, Li-salt: Molecular Probes, Eugene, OR) ranging from 100 μM to 1 mM, a range in which the fluorescence of Lucifer yellow is a linear function of dye concentration (Atkinson & Sheridan, 1988). In some experiments, 250 μM rhodamine-labeled dextran (mol wt 10,000, Molecular Probes) was included with the Lucifer yellow in the pipette. After a seal was made on a cell pair or cluster, spread of Lucifer yellow was monitored with a low light level Cohu video camera (5000 series) using a SIT image tube and having adjustable gain, high voltage, and black level. Fluorescence intensity of Lucifer yellow was monitored continuously by recording the SIT camera output on a Panasonic Ag-6200 VCR. Neutral density filters with ODs between 0.5 and 1 were used to reduce the excitation light intensity from a high pressure Nikon mercury lamp. A Nikon fluorescein filter with a

460–485-nm excitation filter and a 515–545-nm barrier filter or a rhodamine filter with a 535–550 nm excitation filter and a 580-nm barrier filter were used. The rhodamine filter was used only at the end of the experiment to check if the rhodamine-labeled dextran had spread to any adjacent cells. The videotaped images were then digitized using an ETM image processor and VideoProbe software (Version 1.0., Mission Viejo, CA). Frames were digitized no faster than every 2 sec, but at least eight frames were averaged together to give the digitized image. VideoProbe software was then used to obtain a plot of fluorescence intensity *versus* time for each cell in the cell pair or cluster: the region of the cell used for measurement was defined by placing a small rectangle in the center of the digitized cell image. The intensity was determined from the average pixel value in this rectangle.

pH Experiments

To test for the effect of pH on junctional permeability, 3 ml of sodium acetate solutions of pH 6.0, 6.4, 6.76, and 7.4 were perfused into the external bath just before the patch electrode was introduced into the bath. Seals were formed about 5–7 min after start of perfusion. Lowering of the internal pH has been observed within this time in sheep cardiac Purkinje strands (De Hemptinne, Marrannes & Vanheel, 1983). Transfer of dye was then assayed 5 min later (sufficient time for dye transfer in untreated cells). After 10–15 min, mammalian Ringer or an ammonia solution was perfused into the external bath in an unsuccessful attempt to raise the intercellular pH back to normal levels (*see* Discussion).

Electrophysiology

Electrophysiological recordings were made with two Axopatch 1-C patch clamps (Axon Instruments, Foster City, CA) with headstages mounted on two sets of three orthogonal positioners (Newport, Fountain Valley, CA) attached to an inverted Nikon (A.G. Heinze, Irvine, CA) microscope with Hoffman optics. The clamps were driven by data acquisition programs written in FORTRAN by J.E. Hall for the IBM personal computer driving the Adlab data acquisition board (Interactive Microwave, PA). Data were stored on floppy disk, transferred to ASCII format and imported into LOTUS, QUATTRO, or QUATTROPRO for analysis. Data were also translated to Axon Instruments PCLAMP (Axon Instruments, Foster City, CA) compatible files by software written in QUICK BASIC by G.R. Ehring and L. Rioni. PCLAMP software was used to obtain the time constants shown in Fig. 10. The data were filtered either by a filter built into the patch clamp or by an 8-pole Bessel filter (Frequency Devices, Haverhill, MA). Unless otherwise indicated the data were filtered at 2 kHz. The current traces shown in this paper were not leak subtracted.

Solutions

Cell Preparation

TD buffer contained: 140 mM NaCl, 5 mM KCl, 700 μM Na_2SO_4, 5 mM glucose, and 25 mM Tris base, pH to 7.4 with HCl.

Patch Clamping

Internal. Solution contained (in mM): 160 KAsp, 1.1 EGTA, 2 $MgCl_2$, 0.1 $CaCl_2$, 10 HEPES, and 5 ATP, pH to 7.2 with KOH.

External. Mammalian Ringer contained (in mM): 140 NaCl, 4.5 KCl, 2 $CaCl_2$, 1 $MgCl_2$, 5 HEPES and 5 glucose, pH to 7.4 with NaOH. K Ringer contained (in mM): 160 KCl, 2 $CaCl_2$, 1 $MgCl_2$, 10 HEPES, and 5 glucose, pH to 7.4 with KOH. 80/80 Na/K contained (in mM): 80 NaCl, 80 KCl, 2 $CaCl_2$, 1 $MgCl_2$, 10 HEPES, and 5 glucose, pH to 7.4 with KOH.

pH Experiments

pH 7.4 and 6.76 solutions contained (in mM): 140 NaCl, 4.5 KCl, 2 $CaCl_2$, $MgCl_2$, 5 HEPES, 5 glucose, and 20 Na acetate, pH adjusted with NaOH. pH 6.0 and 6.4 solutions contained in (mM): 70 NaCl, 4.5 KCl, 2 $CaCl_2$, 1 $MgCl_2$, 5 MES, 5 glucose, and 90 Na acetate, pH adjusted with NaOH.

For double patch-clamp experiments the internal solution was the same as for single patch-clamp experiments except that there was no ATP.

For dye studies stock solutions of Lucifer yellow were diluted into the above internal solution without ATP. In some cases the dye solution was filtered through a 0.5-μm FH-type Millipore filter.

Results

Morphology

Figure 2 shows a typical preparation of cells obtained immediately following trypsin digestion of whole embryonic lenses. Two types of cells can be distinguished: roughly spherical cells, varying from 2–16 μm in diameter, and elongated cells, about 5–10 μm in width and about 100 to 200 μm in length. The elongated cells rarely stuck to the bottom of the dish, and the majority of them disappeared 2–3 hr after incubation at 37°C, 5% CO_2. They were mostly found in large clusters (hundreds of cells), occasionally in groups of two to five, and rarely as single cells. Since the spherical cells readily attached to coated glass chambers, they were chosen for initial assessments of membrane permeability properties of dissociated lens cells.

A nuclear stain was used in order to determine whether the spherical cells were actually cells or just vesicular fragments, possibly of the longer cells. We found that all of the spherical cells on the dish, regardless of size, including those in clusters or pairs, contained nuclei (Fig. 3).

Dissociated embryonic chick lens cells were pelleted and freeze fractured, and thin section electron microscopy was performed (*data not shown*). The pellet of cells contained both spherical and

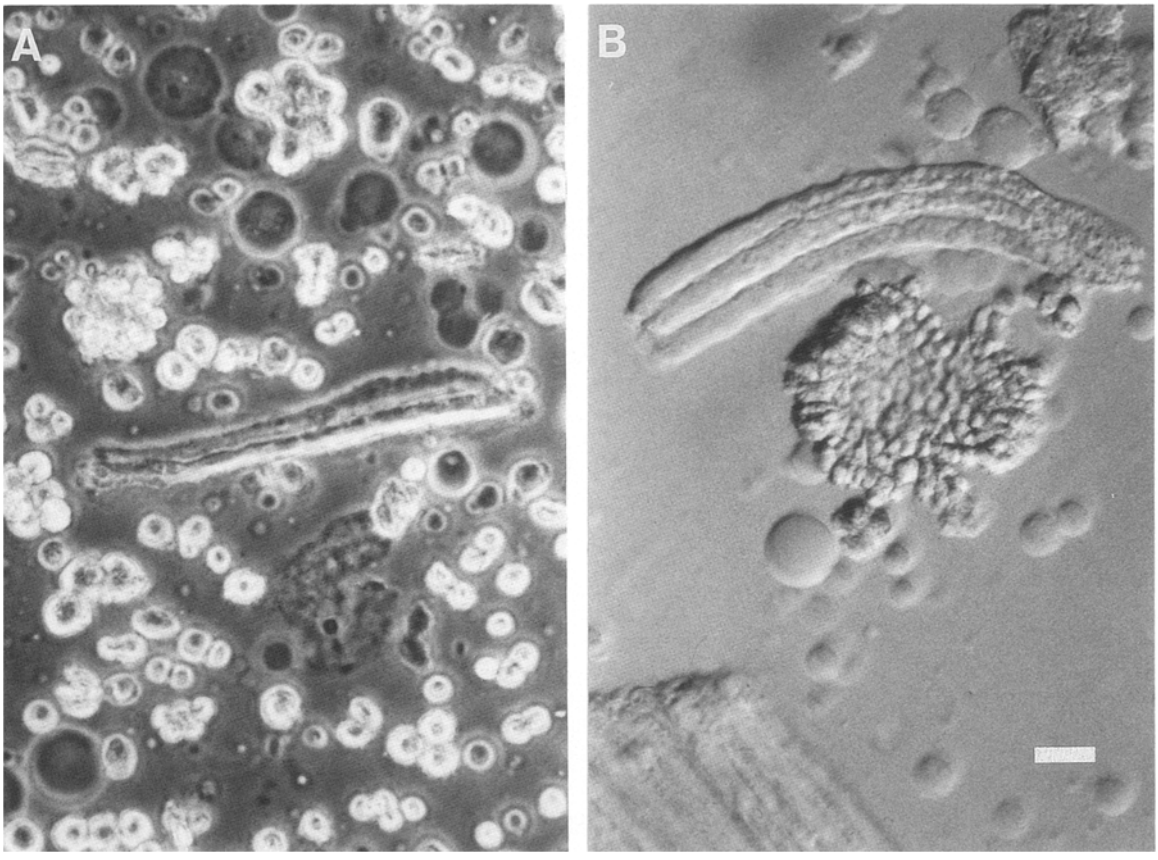

Fig. 2. (*A*) Light micrograph, taken just after dissociation, of spherical cells from lenses from a 12-day-old embryo (phase contrast). (*b*) Light micrograph, taken just after dissociation, of a fiber-like cluster of three cells from an 11-day-old embryo (Hoffman optics). Scale bar is 20 μm.

elongated cells. Many of the cells were connected by gap junctions composed of small crystalline arrays of particles. These regions are similar to gap junction plaques from the anterior epithelium (Goodenough, Dick & Lyons, 1980). The more elongated cells contained cytoplasm filled with amorphous crystalline proteins. They contained gap junction regions and, in addition, more extensive junctions composed of intramembrane particles, loosely packed. This latter array is similar to arrays found in fiber-cell junctions (Zampighi et al., 1989).

Cell-to-Cell Permeability

Dye Spread

To assess the cell-to-cell permeability of the spherical cells, Lucifer yellow and a rhodamine-labeled dextran were co-injected via a patch pipette into one cell of a cell pair or a cluster. In 44 out of 49 cells (90%), detectable amounts of Lucifer yellow passed to the adjacent cell within 1 or 2 min. In 12 out of 14 experiments, no rhodamine-labeled dextran was observed in an adjacent cell up to 30 min after injection (Fig. 4). In 2 out of 14 cases, slight fluorescence, possibly due to membrane leak, was observed in the cell adjacent to the cell attached to the patch pipette. These experiments demonstrate that cells from the dissociated preparation are coupled by communicating pores (presumably gap junction channels) which restrict the passage of large molecules.

An advantage of using the patch-clamp technique to inject dye into the cell is that the permeability of the single membrane and the spread of dye can be monitored simultaneously. Gigaohm seals were routinely obtained with low concentrations of Lucifer yellow in the pipette. With the appropriate neutral density filter and a high sensitivity SIT camera it was possible to quantify dye movement. Figure 5*A* shows that the dye moved rapidly from the injected cell to the adjacent cell, indicating that these cells were well coupled. Figure 5*B* shows that although the membrane resistance does decline dur-

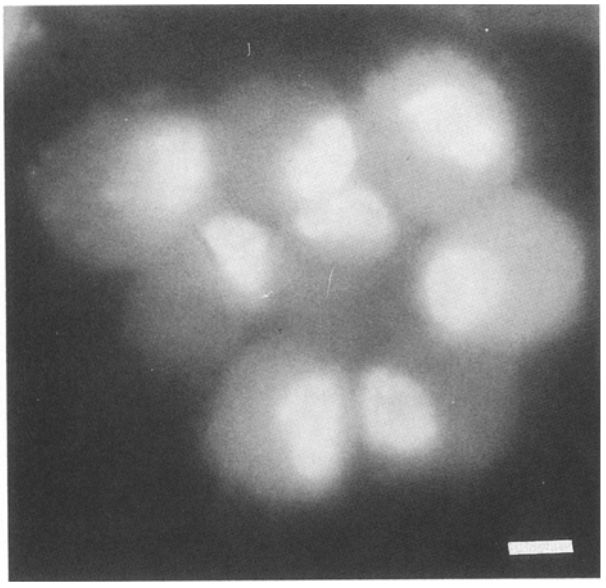

Fig. 3. Nuclear staining of a cluster of eight cells, showing rounded nuclei. Cells were fixed in 4% paraformaldehyde, then stained with 50 μg/ml Hoescht dye 33258 (Aldrich Chemical, Milwaukee, WI) and viewed on a Zeiss III RS noninverted microscope with UV filter. Scale bar is 8 μm.

ing dye injection, it remains relatively high over a period of time long enough to permit quantitative evaluation of the spread of dye. Figure 5*C* shows a decline in the junctional conductance during the period over which dye spread is measured. However, since the decline is less than about 10%, a reasonable value for the effective diffusion rate can be calculated.

Junctional Conductance

Junctional conductance was measured in double patch-clamp experiments, in which each cell of a pair was clamped in the whole-cell mode. Immediately after break-in to whole cell mode in both cells, the junctional conductance was large. There was no voltage dependence of the cell-to-cell current for the range of −50 to 90 mV transjunctional voltage (Fig. 6*A*). This linear voltage relationship held for all cell pairs tested. The cell-to-cell conductance declined during the course of the experiment, and in some instances (two cell pairs), apparent unitary junctional currents, with a single-channel conductance between 200–300 pS (mean = 286.3 ± 38), were observed (Fig. 6*B*). All single cell-to-cell conductance measurements were done between 50 and 80 mV transjunctional voltage. A similar decline in cell-to-cell conductance has been found in rat lacrimal glands (Neyton & Trautmann, 1985).

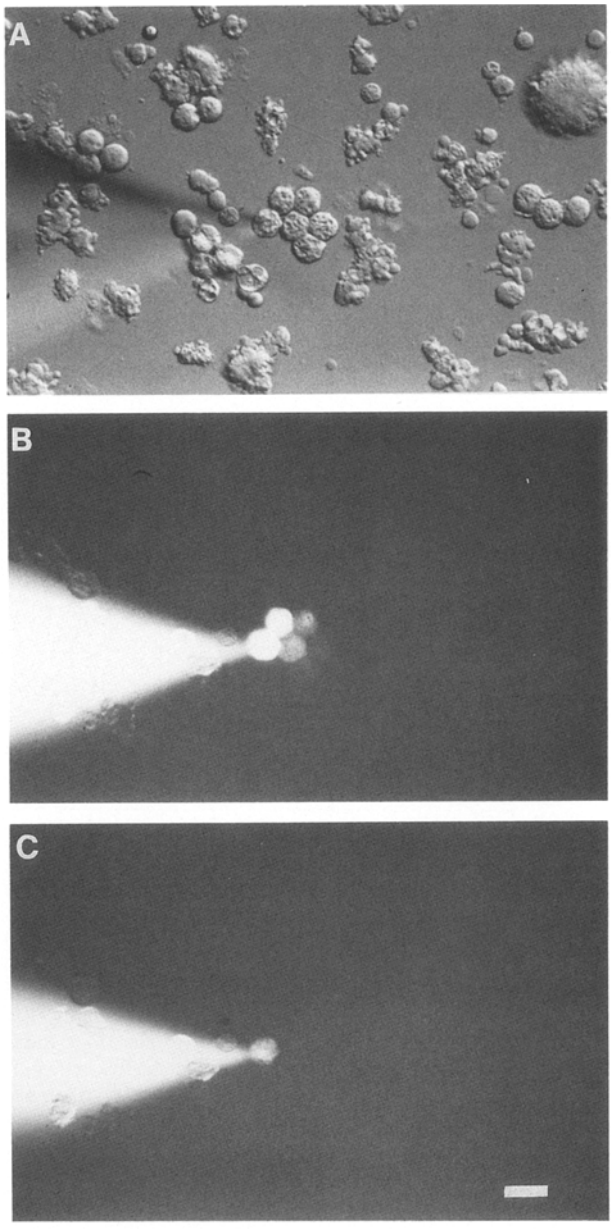

Fig. 4. Light micrograph of a typical dye injection experiment. The patch pipette contained Lucifer yellow, which spread to adjacent cells, and a rhodamine-labeled dextran, which did not spread to adjacent cells. (*A*) Hoffman optics. (*B*) Fluorescein-filtered image. (*C*) Rhodamine-filtered image. Scale bar is 20 μm.

pH Dependence

The pH dependence of cell-to-cell permeability was investigated by bathing the cells in sodium acetate solutions of different pH. Figure 7 summarizes the results, which indicate that it is possible to block dye transfer when the cells are bathed in a sodium acetate solution of pH 6.0. Coupling was sometimes observed with an external sodium acetate solution of pH 6.4 and always observed with an external

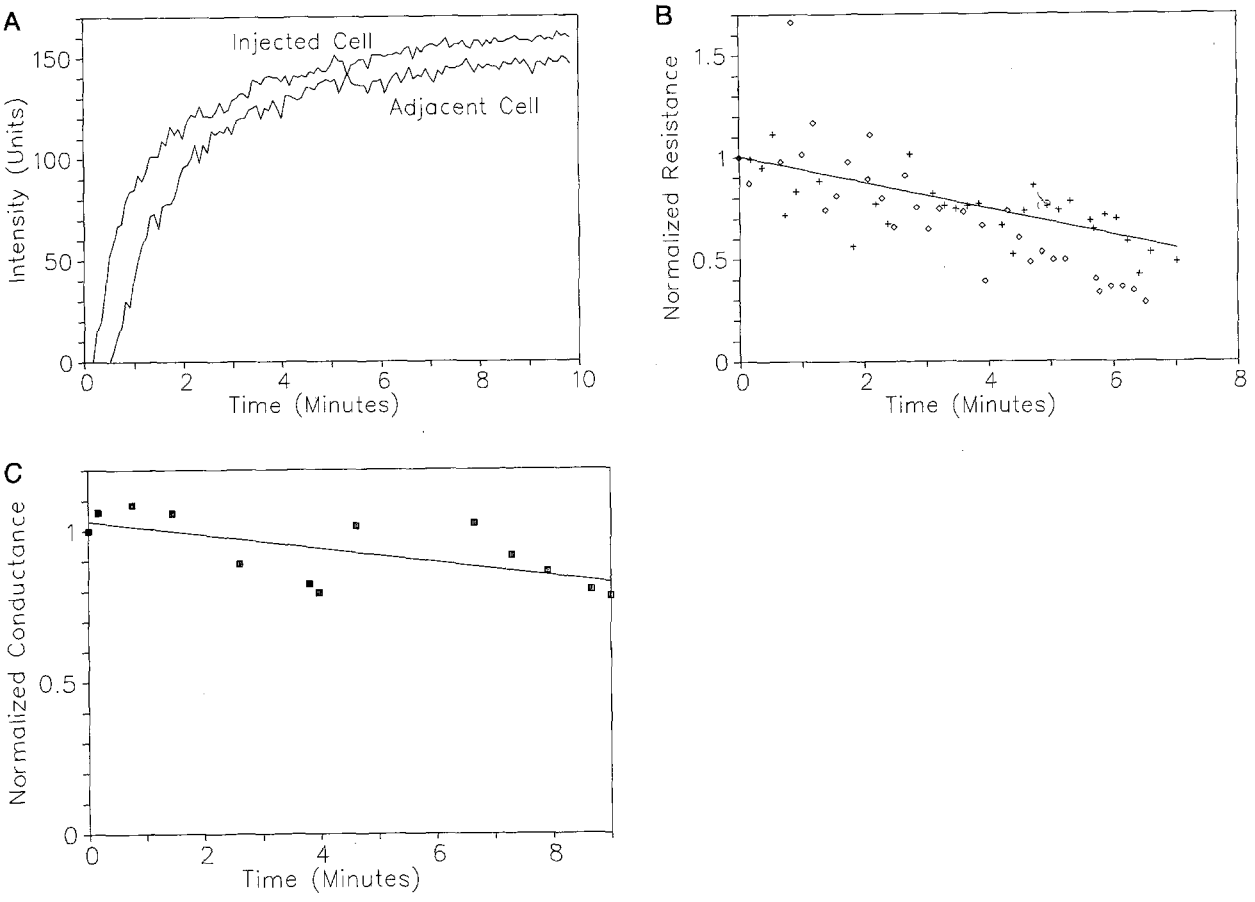

Fig. 5. (*A*) Intensity of dye fluorescence *versus* time for a cell pair injected with Lucifer yellow. Top trace is the cell which was whole-cell clamped, and bottom trace is the adjacent cell. Concentration of Lucifer yellow in the pipette was 437 μM, and the neutral density filter used was 0.7. (*B*) Normalized single-membrane resistance as a function of time for two dye experiments: a cell pair (crosses) and a cluster of six (diamonds). The initial resistances were 9.9 and 2.7 GΩ, respectively. The concentrations of Lucifer yellow in the pipette were 1.1 mM, and 437 μM, respectively. The neutral density filters used were 1 and 0.7, respectively. The solid line is an average of two linear regressions, one for each set of points. The slope (rate of decline of resistance) is −0.06 U/sec. (*C*) Normalized junctional conductance as a function of time during a typical experiment in which each cell of a cell pair was whole-cell clamped. The initial junctional conductance was 39 nS. Each time point is the average conductance calculated from a family of pulses. The initial time corresponds roughly to the time of break-in of the second clamp to whole-cell mode. The line is a linear regression of the data points. The slope (rate of decline of junctional conductance) is −0.02 U/sec.

sodium acetate solution of pH 6.76. Although it was not possible to reverse the block of dye coupling by perfusing in either mammalian Ringer or an ammonia solution at the end of the experiment, it was possible to form a stable seal with external solutions at each pH and thus to measure membrane conductance. There was no nonselective increase in membrane permeability during block of dye spread. Thus, at least by this criterion, the cell remained healthy throughout the experiment.

Since it is the internal pH which is believed to mediate closure of gap junction channels (Scheutze and Goodenough, 1982; Miller & Goodenough, 1986), we wanted to ascertain the change in internal pH due to the externally applied sodium acetate solutions. We have thus measured internal pH using the pH indicator BCECF (Molecular Probes, Eugene OR). Detailed results will be published later; however, for the purpose of the present paper we note that initial measurements indicate that with 20 mM sodium acetate in the external solution, the internal pH is approximately the same as the external pH.

Single-Membrane Permeability

Whole-cell measurements were made of the conductances of single cells, cell pairs and cell clusters. Figure 8 shows a histogram of the membrane input

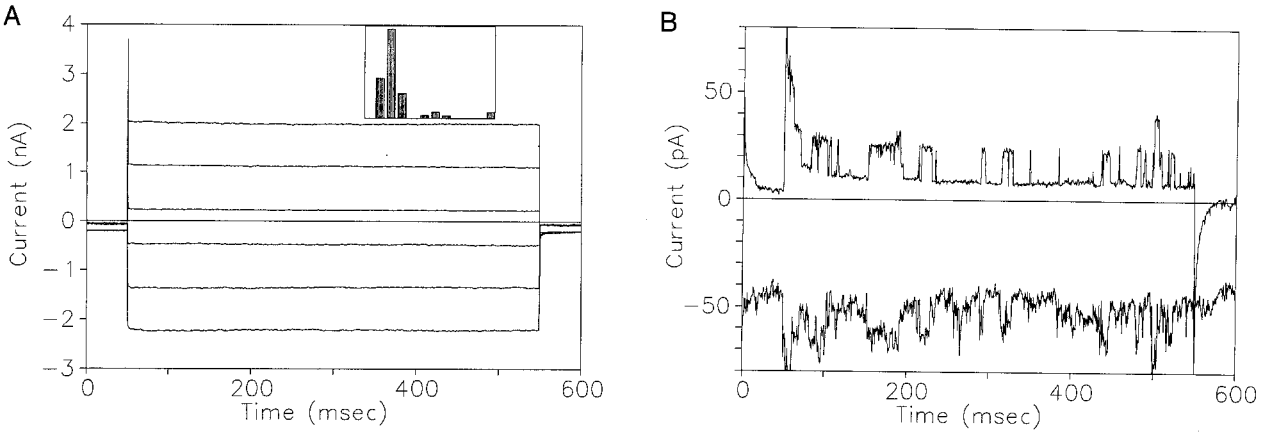

Fig. 6. (*A*) Junctional currents taken from one of the cell pairs analyzed. The top set of three traces represents the current in the active clamp, and the bottom set of three traces represents the current in the passive clamp. If the single-membrane resistances are large, the junctional current is the change in current in the passive clamp (Neyton & Trautmann, 1985). Both clamps were held at −40 mV, and the active clamp was stepped to 10, 30, and 50 mV above the holding potential. Note the capacitative spike in the active-clamp traces and its absence in the passive-clamp traces. The inset shows a histogram of initial junctional resistances during the first 100 sec after break-in of the second clamp to whole-cell mode. Each bar represents a bin 2 × 10^7 Ω wide. Thus the first bin (which is empty) represents junctional resistances from 0 to 2 × 10^7 Ω. The peak bar falls in the range of 4–6 × 10^7 Ω, and the last bin contains junctional resistances from 22–24 × 10^7 Ω. (*B*) Single-channel events found after the junctional current had run down. As in *A*, the top trace represents the current in the active clamp and the bottom trace represents the current in the passive clamp. Both clamps are held at −40 mV, and the active clamp is stepped to 10 mV (the transjunctional voltage is therefore 50 mV). The unitary event is taken as the predominant current step event, even though it appears that there are smaller current steps in the trace. The extra noise in the lower trace is due to an imperfect seal, or noisy conductance, in the second cell. However, this noise does not depend on the voltage in the driven cell and adds to the junctional current which, in this case, is most clearly seen in the driven cell. Note: a positive transjunctional voltage corresponds to a positive voltage applied to the active clamp and a negative transjunctional voltage corresponds to a negative voltage applied to the active clamp.

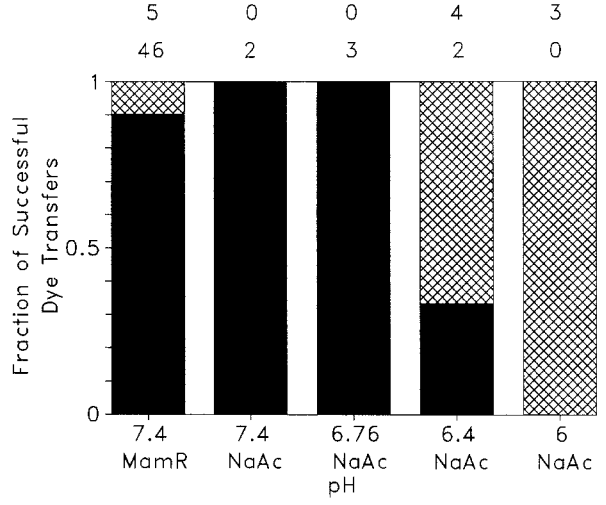

Fig. 7. A composite histogram of the pH dependence of junctional permeability. The bottom set of bars (solid) shows the fraction of events in which the dye passed to the adjacent cell. The top set of bars (crosshatched) shows the fraction of events in which the dye did not spread to the adjacent cells. The events at each pH were normalized to the total number of events at that pH. The number of observations is indicated above the plot. *MamR* = mammalian Ringer. *NaAc* = sodium acetate solutions.

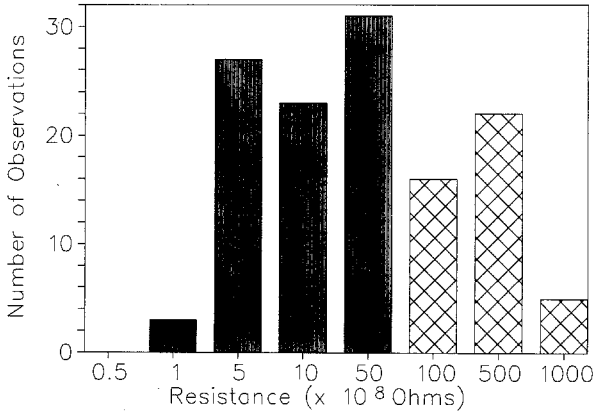

Fig. 8. The membrane resistances for all single cells, cell pairs, and clusters tested, both with and without dye. This resistance is calculated as the slope of the linear part of an *I-V* ramp at −80 mV. Ramp speed was 200 mV/sec. The average membrane resistance was 7.9 GΩ. Note that the values in excess of 10 GΩ (crosshatched bars) probably reflect the seal resistance and are thus lower bounds on the actual membrane resistance.

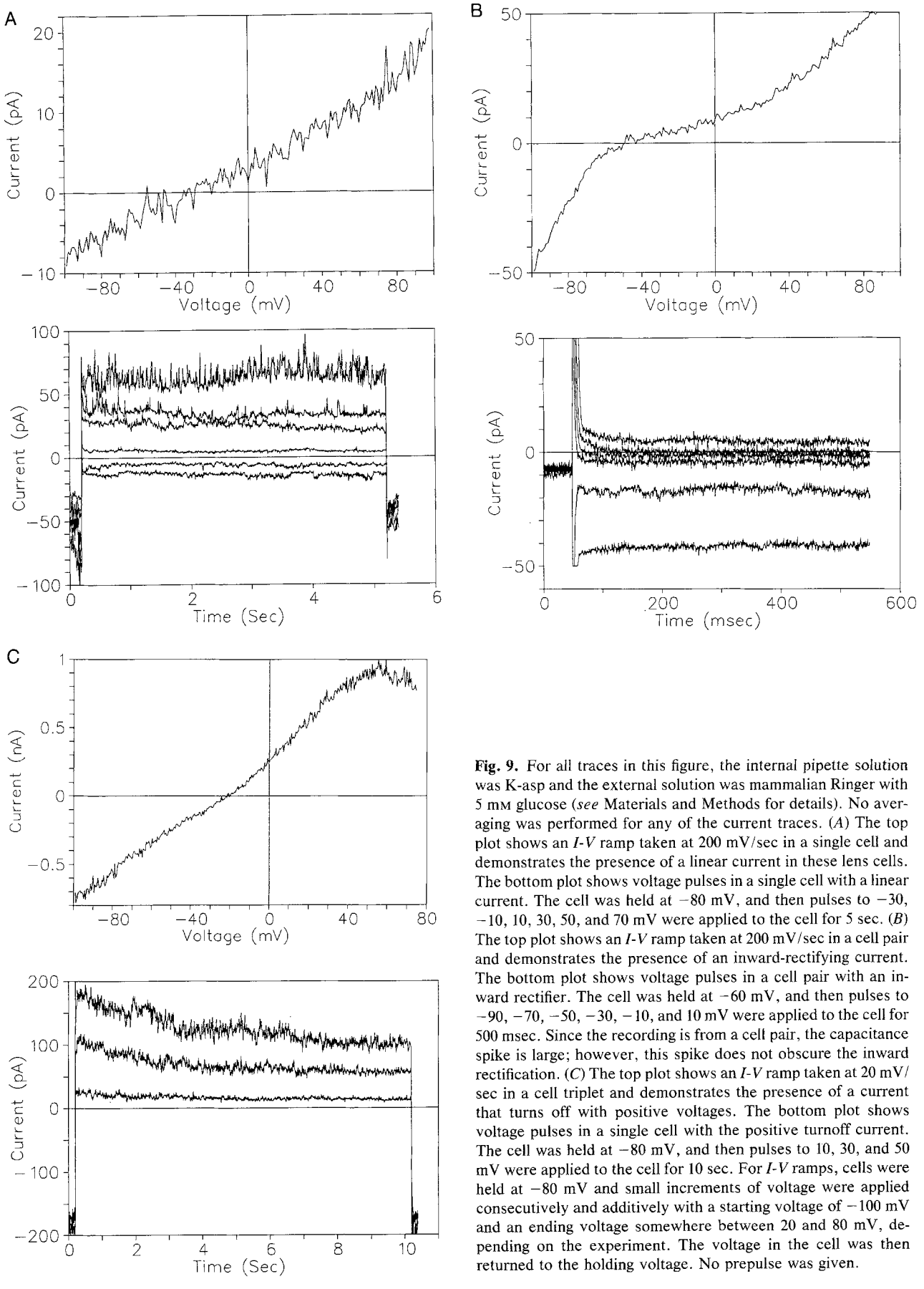

Fig. 9. For all traces in this figure, the internal pipette solution was K-asp and the external solution was mammalian Ringer with 5 mM glucose (*see* Materials and Methods for details). No averaging was performed for any of the current traces. (*A*) The top plot shows an *I-V* ramp taken at 200 mV/sec in a single cell and demonstrates the presence of a linear current in these lens cells. The bottom plot shows voltage pulses in a single cell with a linear current. The cell was held at −80 mV, and then pulses to −30, −10, 10, 30, 50, and 70 mV were applied to the cell for 5 sec. (*B*) The top plot shows an *I-V* ramp taken at 200 mV/sec in a cell pair and demonstrates the presence of an inward-rectifying current. The bottom plot shows voltage pulses in a cell pair with an inward rectifier. The cell was held at −60 mV, and then pulses to −90, −70, −50, −30, −10, and 10 mV were applied to the cell for 500 msec. Since the recording is from a cell pair, the capacitance spike is large; however, this spike does not obscure the inward rectification. (*C*) The top plot shows an *I-V* ramp taken at 20 mV/sec in a cell triplet and demonstrates the presence of a current that turns off with positive voltages. The bottom plot shows voltage pulses in a single cell with the positive turnoff current. The cell was held at −80 mV, and then pulses to 10, 30, and 50 mV were applied to the cell for 10 sec. For *I-V* ramps, cells were held at −80 mV and small increments of voltage were applied consecutively and additively with a starting voltage of −100 mV and an ending voltage somewhere between 20 and 80 mV, depending on the experiment. The voltage in the cell was then returned to the holding voltage. No prepulse was given.

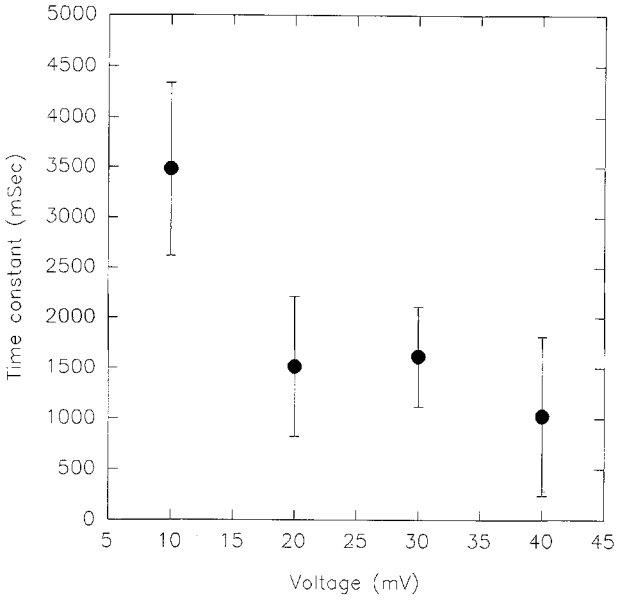

Fig. 10. Time constants for all the fits performed on a series of pulses in cells with the voltage-dependent turnoff. Only families of pulses from 0 to 40 mV (absolute voltage) were used (i.e., a single pulse to 40 mV was not averaged in). This figure represents the average of three cells (nine traces).

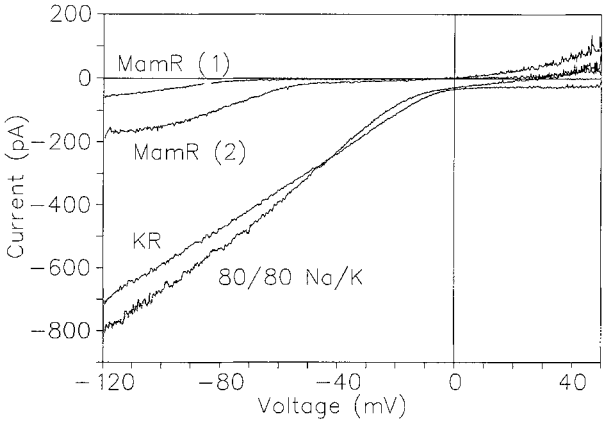

Fig. 11. *I-V* ramps in different solutions (ramp rate is 10 mV/sec). The cell was whole-cell clamped in mammalian Ringer. The external solution was then changed in the following order: potassium Ringer, 80/80 Na/K, mammalian Ringer. *MamR (1)* = mammalian Ringer before any solution change. *KR* = potassium Ringer. 80/80 *Na/K* = Ringer's solution with 80 mM NaCl and 80 mM KCl. *MamR (2)* = mammalian Ringer after all solution changes.

resistances (calculated as the slope of *I-V* ramps at −80 mV) of all cells tested. The median input resistance without dye in the pipette was 7.05 ± 0.29 GΩ; with dye the resistance measured was 7.9 ± 0.96 GΩ. These results indicate that dissociated embryonic chick lens cells are very tight electrically and that the dye has little effect on membrane resistance.

Three types of currents were observed in the population of lens cells tested: a voltage-independent "leak" (63% of the cells tested); an inward rectifier, turning on at about −50 mV (14% of the cells tested); and a current which turns off at positive voltages of about 0–40 mV over a period of seconds (23% of the cells tested). Examples of each of these are shown in Fig. 9. The cells which showed the voltage-dependent turnoff had much higher current levels than cells which did not.

The time course of the voltage-dependent turnoff was investigated further by fitting the current traces to a single-exponential function. The time constant calculated from the exponential fits was found to be slightly voltage dependent (Fig. 10).

Selectivity experiments were performed on both the linear current and the inward rectifier. In nine experiments, the linear current showed no selectivity to potassium or chloride. In two experiments the inward rectifier was shown, as expected, to be selective for potassium (Fig. 11).

Discussion

Understanding the relationship between membrane permeability and lens transparency requires a detailed knowledge of the membrane permeability properties of all the different cell types in the lens. This paper describes single-membrane currents and cell-to-cell conductances in dissociated cells from developing chick lenses.

The embryonic lens has a higher percentage of differentiating cells and immature fiber cells than do adult lenses, and to date no whole-cell clamping has been reported on nonepithelial cells. We have not found a good biochemical marker to distinguish between epithelial and nonepithelial cells. However, since there is a dramatic increase in cell size as the epithelial cells differentiate into fiber cells, cell volume could be used to indicate cell type. No data is available for the exact dimensions of embryonic chick lens fiber cells. However, if we assume that a mature fiber cell in the cortex spans the thickness of the lens (from anterior to posterior), then reasonable dimensions for a 9–15 day embryonic chick lens cortical fiber cell would be $2 \times 5 \times 10^3 = 10 \times 10^3$ μm^3. A spherical cell of this volume would have a radius of 13.5 μm. The largest dissociated cells had radii of about 8 μm. Thus it seems unlikely that the dissociated cells being studied are mature fiber cells which have become spherical. However, fiber-cell length decreases from the cortex towards the equator, and thus the possibility exists that some of the spherical cells tested might come from regions

just beyond the epithelial layer, the so-called transition zone (Fig. 1).

The junctional conductance measurements of embryonic chick lens gave results similar to those of Cooper et al. (1989) for the adult frog lens. The majority of the values of junctional resistances reported here fall within the same range as the majority of junctional resistance values reported in their histogram (Fig. 8 in Cooper et al., 1989), and the junctional currents are voltage independent over similar ranges. These results suggest that there is little difference in junctional conductance between dissociated adult frog epithelial cells and dissociated embryonic chick lens cells. This similarity is interesting in light of the very different junctional morphology between chick lenses and frog lenses (Lo & Harding, 1986). In particular, Lo and Harding (1986) report a 100% occurrence of gap junction arrays with randomly arranged particles in the adult frog epithelium, whereas freeze-fracture studies on the dissociated embryonic chick lenses in our preparation show the presence of what Lo and Harding termed crystalline arrays.

Cooper et al. (1989) report a single cell-to-cell conductance of 118 pS, compared to our value of 286 pS. One possibility for this discrepancy is the species difference between frog and chicken. Alternatively, the difference could be attributed to a change in gap junction channel type during development, since Cooper et al. (1989) used adult frog lenses. There is no evidence for a change in the protein composition of lens gap junctions during development; however, pH sensitivity has been shown to markedly decrease during the embryonic development of the lens (Scheutze & Goodenough, 1982).

The pH blocking experiments are in agreement with junctional permeability studies done in different lens preparation (Scheutze & Goodenough, 1982; Miller & Goodenough, 1986). Subsequent photobleaching experiments (to be published in detail later) indicate that the pH block of junctional permeability in dissociated embryonic chick lens cells is reversible. The irreversible block found here could arise from our inability to restore the internal pH to pH 7.2 due to the large buffering capacity of the patch pipette which, after perfusion of the low pH solutions, would presumably contain sufficient diffusion-trapped acetate anions to render the kinetics of proton removal much slower than the kinetics of acidification.

Only one other paper reports data on whole-cell currents from freshly dissociated lens cells. Cooper et al. (1989) showed that most epithelial cells dissociated from adult frog lens have very little current (1.5 GΩ membrane resistance) and that except for an outward-rectifying current that is blocked by barium, all currents are voltage independent over the range of −100 to 20 mV. We do not find this outwardly rectifying current in chick lens, but we do find a large percentage of cells (63%) with high resistance (7 GΩ membrane resistance) voltage-independent currents. In a series of experiments in which the capacitance was measured (*data not shown*), we estimated a specific resistance of 147 kΩ-cm^2 for lens cells with the voltage-independent current. This differs from the value of 12.6 kΩ-cm^2 reported by Cooper et al. (1989). This difference could be due to the age difference between the two preparations used and could possibly imply a decrease in membrane permeability change during the development of the lens. We also report two new whole-cell currents not previously observed in chick lens cells: an inward rectifier and a larger current which turns off with positive voltage (0–40 mV) with a slightly voltage-dependent time constant.

An inward rectifier, found in cell-attached patches from chick lens epithelium (Rae, 1986) has a conductance of 30 pS. Assuming E_K is −80 mV, then at −100 mV this would give rise to 0.6 pA of current. Furthermore, using an open probability of 0.2 at −100 mV (Rae, 1986) and the data from the pulses in Fig. 9*b* of this paper, there would be about 417 channels for the cell pair or about 209 channels for a single cell. Rae (1986) routinely observed 6–8 inward-rectifier channels in cell-attached patches. Assuming a cell radius of 4 μm (average size) and an average patch size of 1 μm^2, there would be 1206 channels per cell in Rae's preparation. The discrepancy between Rae's results and ours could be due to either washout of the channels upon equilibration of the pipette contents with the cell or to effects on the inward rectifier as a result of treatment of the cells with trypsin. However, another possibility is that the neighboring cells in the epithelial sheet supply a factor or factors necessary to keep this channel open. Since the channel number is small and the open probability low, a single cell might not show enough current to be able to clearly identify the inward rectifier (20 pA for 37 channels for the case in Fig. 9*b*, but perhaps less current in other single cells). Thus whole-cell clamping of more than one cell has the advantage of increasing the probability of observing low density channels.

On a macroscopic level, the inward rectifier reported here is similar in voltage dependence and selectivity to the inward rectifier found in whole-cell recordings of dissociated epithelial cultures from human, rabbit, mouse and rat (Cooper, Rae & Dewey, 1991). We found the inward rectifier in only 14% of the cells tested, whereas Cooper et al. (1991) found the inward rectifier in most cells in rabbit, rat, and mouse epithelial explants. It is interesting that Cooper et al. (1991) found the inward rectifier in

only a small number of cells from human epithelial explants. The physiological role of this channel in dissociated chick lens cells is unclear. However, there is speculation that it might work together with the Na^+-K^+ pump to prevent accumulation of potassium inside the cell (Cooper et al., 1991). More experiments are needed to evaluate the physiological role of this channel and to determine if in fact the inward rectifier can serve as a marker for cell type.

We have not yet found evidence in any other lens preparation for a current similar to the voltage-dependent turnoff. Although no role can yet be attributed to this current, it is remarkably similar in its voltage dependence and kinetics to currents found when the major intrinsic protein of lens fiber membranes (MIP26) is reconstituted into planar lipid bilayers (Ehring et al., 1990). We feel this similarity warrants further study.

The cell-to-cell permeability studies performed here indicate that all types of dissociated cells from developing chick lenses are well coupled. Single-membrane permeability studies suggest that the lens is made up of a heterogeneous population of cells. It will, we hope, be possible to correlate the observed permeability properties with lens cell type and thus to localize specific permeability properties to regions of different cell type in the lens. Finally, more effective methods for isolating and recording from fiber cells are needed in order to provide a more complete picture of ionic permeabilities in the lens.

The authors would like to thank Mary Hawley for her technical support and for the preparation of Fig. 1, Richard Wetts for his help with the nuclear staining, Mike Kreman for his help with Fig. 3 and Ruth Davis for helpful comments on this manuscript. This work was supported by NIH grants EY-06884 to JEH and EY-04110 to GAZ.

References

Atkinson, M.M., Sheridan, J.D. 1988. Altered junctional permeability between cells transformed by *v-ras, v-mos,* or *v-src*. *Am. J. Physiol.* **255:**C674–C683

Bunce, G.E., Kinoshita, J.H., Horwitz, J. 1990. Nutritional factors in cataract. *Annu. Rev. Nutr.* **10:**233–254

Cooper, K, Gates, P., Rae, J.L., Dewey, J. 1990. Electrophysiology of cultured human lens epithelial cells. *J. Membrane Biol.* **117:**285–298

Cooper, K.E., Rae, J.L., Dewey, J. 1991. Inwardly rectifying potassium current in mammalian lens epithelial cells. *Am. J. Physiol.* **261:**C115–C123

Cooper, K., Rae, J.L., Gates, P. 1989. Membrane and junctional properties of dissociated frog lens epithelial cells. *J. Membrane Biol.* **111:**215–227

Cooper, K.E., Tang, J.M., Rae, J.L., Eisenberg, R.S. 1986. A cation channel in frog lens epithelia responsive to pressure and calcium. *J. Membrane Biol.* **93:**259–269

De Hemptinne, A., Marrannes, R., Vanheel, B. 1983. Influence of organic acids on intracellular pH. *Am. J. Physiol.* **245:**C178–C183

Duncan, G., Bushell, A.R. 1975. Ion analyses of human cataractous lenses. *Exp. Eye Res.* **20:**223–230

Duncan, G., Bushell, A.R. 1979. Relationships between colour, sodium and protein content in individual senile human cataractous lenses. *Ophthalmic Res.* **11:**397–404

Duncan, G., Jacob, T.J.C. 1984. Calcium and the physiology of cataract. *In:* Human Cataract Formation. J. Nugent and J. Whelan, editor. pp. 132–152. Pitman, Bath, UK

Duncan, G., Stewart, S., Prescott, A.R., Warn, R.M. 1988. Membrane and junctional properties of the isolated frog lens epithelium. *J. Membrane Biol.* **102:**195–204

Ehring, G.R., Zampighi, G.A., Horwitz, J., Bok, D., Hall, J.E. 1990. Properties of channels reconstituted from the major intrinsic protein of lens fiber membranes. *J. Gen. Physiol.* **96:**631–664

Goodenough, D.A., Dick, J.S.B., Lyons, J.E. 1980. Lens metabolic cooperation: A study of mouse lens permeability visualized with freeze-substitution autoradiography and electron microscopy. *J. Cell Biol.* **86:**576–589

Jacob, T.J.C. 1986. The electrophysiology of cultured human lens epithelial cells. *J. Physiol.* **377:**39P

Jacob, T.J.C., Bangham, J.A., Duncan, G. 1985. Characterization of a cation channel on the apical surface of the frog lens epithelium. *Q. J. Exp. Physiol.* **70:**403–421

Lo, W.K., Harding, C.V. 1986. Structure and distribution of gap junctions in lens epithelium and fiber cells. *Cell Tissue Res.* **214:**253–263

Mathias, R.T., Rae, J.L. 1985*a*. Steady state voltages in the frog lens. *Curr. Eye Res.* **4:**421–430

Mathias, R.T., Rae, J.L. 1985*b*. Transport properties of the lens. *Am. J. Physiol.* **249:**C181–C190

Mathias, R.T., Rae, J.L., Ebihara, L., McCarthy, R.T. 1985. The localization of transport properties in the frog lens. *Biophys. J.* **48:**423–434

Menko, A.S., Klukas, K.A., Liu, T.F., Quade, B., Sas, D.F., Preus, D.M., Johnson, R.G. 1987. Junctions between lens cells in differentiating cultures: Structure, formation, intercellular permeability, and junctional protein expression. *Dev. Biol.* **123:**307–320

Miller, A.G., Hall, J.E., Zampighi, G.A. 1990. Cell-to-cell permeability in dissociated embryonic chicken lenses. *Biophys. J.* **57:**245*a*

Miller, T.M., Goodenough, D.A. 1986. Evidence for two physiologically distinct gap junctions expressed by the chick lens epithelial cell. *J. Cell Biol.* **102:**194–199

Neyton, J., Trautmann, A. 1985. Single-channel currents of an intercellular junction. *Nature* **317:**331–335

Patmore, L., Duncan, G. 1981. The physiology of lens membranes. *In:* Mechanisms of Cataract Formation in the Human Lens. G. Duncan, editor. pp. 193–218. Academic, San Francisco

Rae, J.L. 1985. The application of patch clamp methods to ocular epithelia. *Curr. Eye Res.* **4:**409–420

Rae, J.L. 1986. Potassium channels from chick lens epithelium. *Fed. Proc.* **45:**2718–2722

Rae, J.L., Cooper, K.E. 1989. Potassium channels in chick lens epithelium change with maturation. *Lens Eye Toxicol. Res.* **6:**833–843

Rae, J.L., Dewey, J., Rae, J.S., Cooper, K.E. 1990. A maxi calcium activated potassium channel from chick lens epithelium. *Curr. Eye Res.* **9:**847–861

Rae, J.L., Levis, R.A. 1984. Patch voltage clamp of lens epithelial cells: Theory and practice. *Mol. Physiol.* **6:**115–162

Robinson, K.R., Patterson, J.W. 1983. Localization of steady currents in the lens. *Curr. Eye Res.* **2:**843–847

Scheutze, S.M., Goodenough, D.A. 1982. Dye transfer between cells of the embryonic chick lens becomes less sensitive to CO_2 with development. *J. Cell Biol.* **92:**694–705

Shinohara, T., Piatigorsky, J. 1977. Regulation of protein synthesis, intracellular electrolytes and cataract formation in vitro. *Nature* **270:**406–411

Stewart, S., Duncan, G., Marcantonio, J.M., Precott, A.R. 1988. Membrane and communication properties of cultured human lens epithelial cells. *Invest. Ophthalmol. Vis. Sci.* **29:**1713–1725

Unakar, N.J., Tsui, J.Y. 1980. Sodium-potassium-dependent ATPase 1. Cytochemical localization in normal and cataractous rat lenses. *Invest. Ophthalmol. Vis. Sci.* **19:**630–641

Wind, B.E., Walsh, S., Patterson, J.W. 1988. Equatorial potassium currents in lenses. *Exp. Eye Res.* **46:**117–130

Zampighi, G.A., Hall, J.E., Ehring, G.R., Simon, S.A. 1989. The structural organization and protein composition of lens fiber junctions. *J. Cell Biol.* **108:**2255–2276

Received 10 December 1991